American Journal of Human Genetics, Volume *92*

Supplemental Data

Mutations in *B3GALT6* that Encodes a Glycosaminoglycan Linker Region Enzyme Cause a Spectrum of Skeletal and Connective Tissue Disorders

Masahiro Nakajima, Shuji Mizumoto, Noriko Miyake, Ryo Kogawa, Aritoshi Iida, Hironori Ito, Hiroshi Kitoh, Aya Hirayama, Hiroshi Mitsubuchi, Osamu Miyazaki, Rika Kosaki, Reiko Horikawa, Angeline Lai, Roberto Mendoza-Londono, Lucie Dupuis, David Chitayat, Andrew Howard, Gabriela Ferraz-Leal, Denise Cavalcanti, Yoshinori Tsurusaki, Hirotomo Saitsu, Shigehiko Watanabe, Ekkehart Lausch, Sheila Unger, Luisa Bonafé, Hirofumi Ohashi, Andrea Superti-Furga, Naomichi Matsumoto, Kazuyuki Sugahara, Gen Nishimura, and Shiro Ikegawa

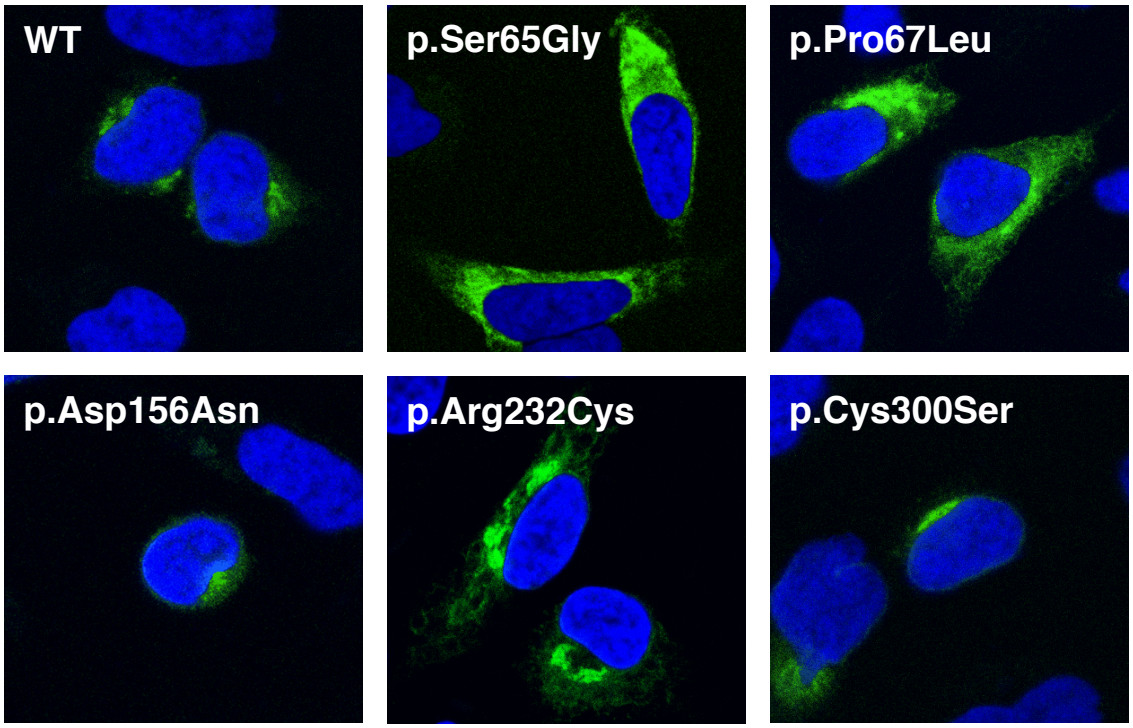

Figure S1. Sub-cellular localization of the missense mutant B3GALT6 proteins

Full-length *B3GALT6* cDNA for the wild type (WT) and missense mutants were cloned into the p3XFLAG-CMV14 vector and were expressed in HeLa cells. Cells were stained with anti-FLAG (green) and 4',6-diamidino-2-phenylindole (DAPI; blue). While WT, p.Asp156Asn and p.Cys300Ser B3GALT6 proteins were localized around nucleus, p.Ser65Gly, p.Pro67Leu and p.Arg232Cys B3GALT6 proteins were localized to cytoplasm.

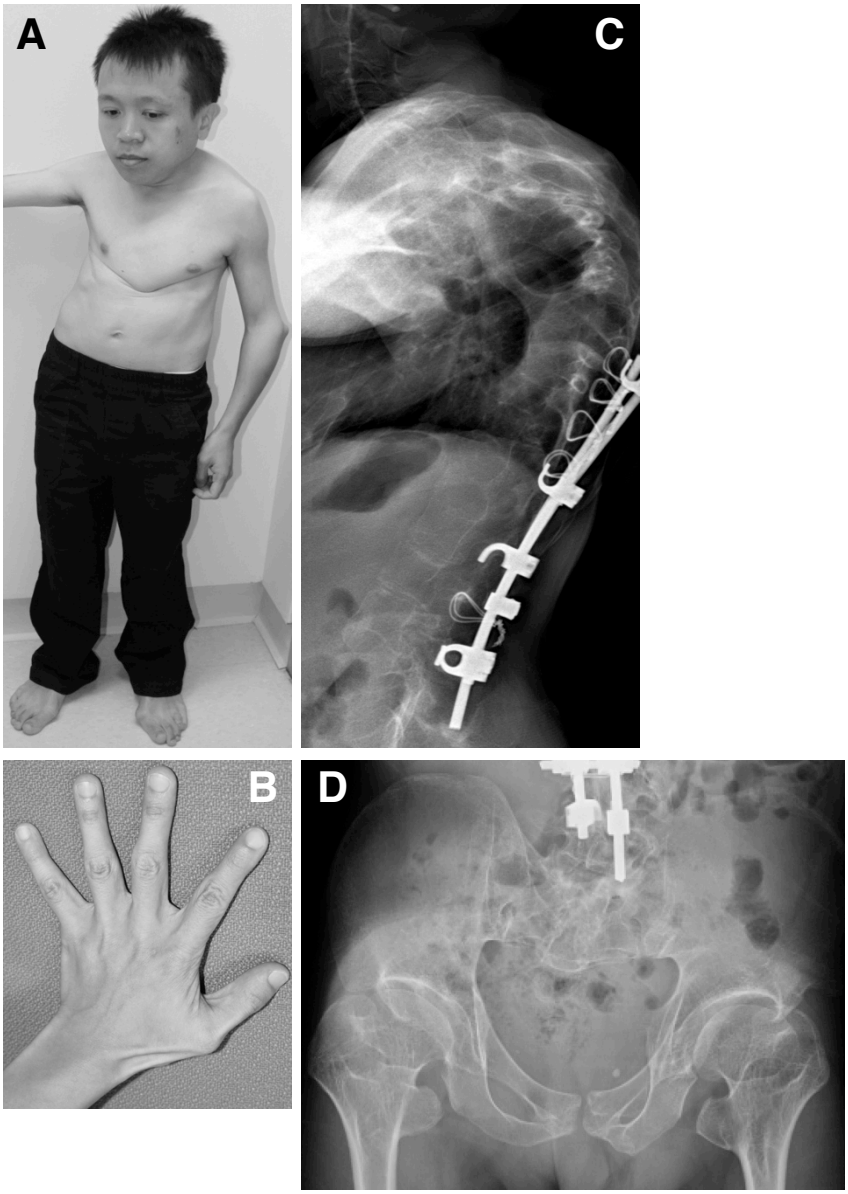

Figure S2. Representative clinical pictures and X-rays for spondyloepimetaphyseal dysplasia with joint laxity 1 (SEMD-JL1) with *B3GALT6* mutations

An individual with SEMD-JL1 (P8) at 34 years of age. **A**, **B**: clinical pictures. The individual had normal facies and intelligence, short trunk-short stature, protruded sternum and elbow deformities. He had no muscle hypotonia, skin problems and hand abnormalities. **C**: Lateral spine X-ray. Severe kyphoscoliosis. **D**: Hip X-ray showing short ilia, prominent lesser trochanter and short femoral neck.

Figure S3. Representative clinical pictures and X-rays for Ehlers-Danlos syndrome, progeroid form (EDS-PF) with *B3GALT6* mutations

P12. **A**, **B**: clinical pictures at 5 years of age. She showed facial dysmorphism (flat face, prominent eyes and hypoplasia of the middle face with and sagging cheeks), wrinkled skin, muscular hypotonia, elbow deformity and clubfoot. **C**: Lateral spine X-ray at age 8 months showing thoraco-lumbar kyphosis, platyspondyly and anterior beak of vertebral body. **D**, **E**: X-rays of elbow (**D**) and hip (**E**) at age 1 year 6 months. Dislocations of the elbow and the left hip joint, epi-metaphyseal dysplasias of the long tubular bones.

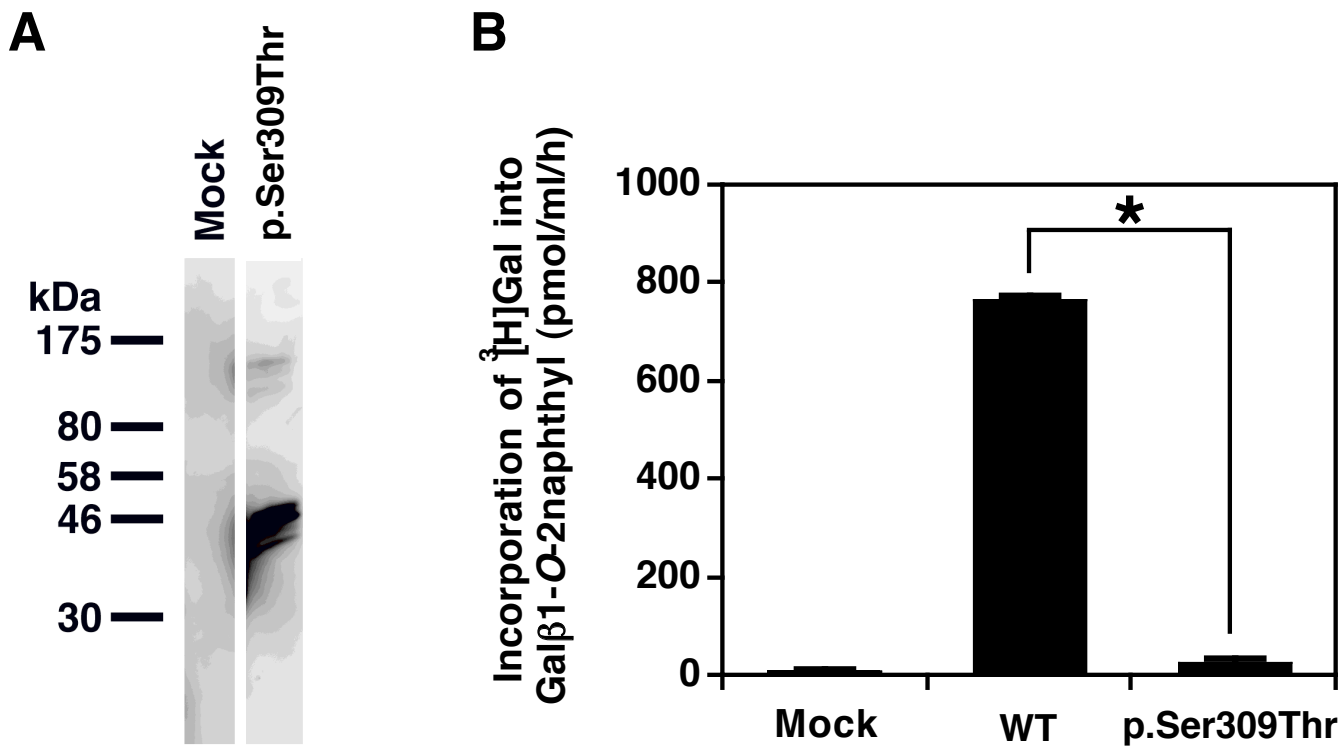

Figure S4. Glycosyltransferase activity of the recombinant p.Ser309Thr B3GALT6 protein

A: Western blotting of the mutant protein. B: Glycosyltransferase activity. "Mock" represents the conditioned medium transfected without the vector. The enzymatic activity of S309T is significantly decreased. *, $p < 0.0001$ versus wild-type by t-test. n=3.

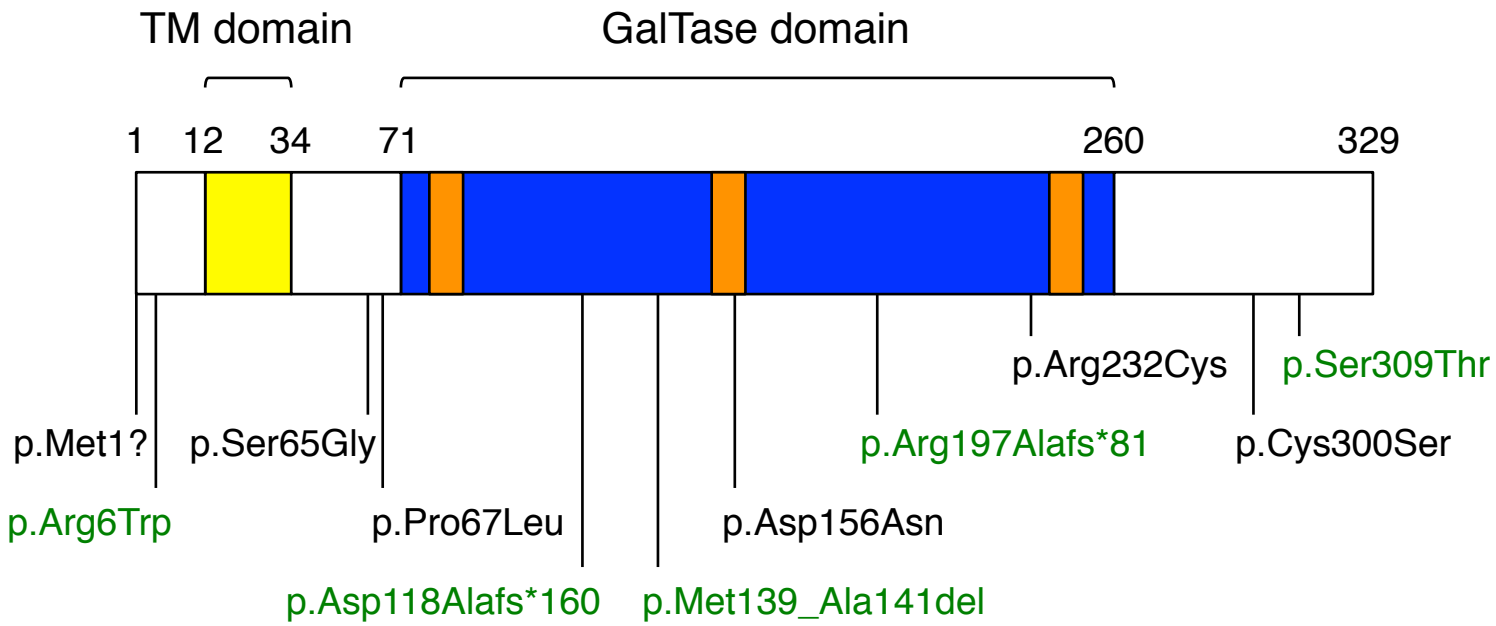

Figure S5. A schematic of B3GALT6 protein and positions of identified mutations

B3GALT6 mutations identified in spondyloepimetaphyseal dysplasia with joint laxity type 1 and Ehlers-Danlos syndrome, progeroid form are indicated by black and green letters, respectively. Functional domains and motifs are color-coded: transmembrane（TM）domain (*yellow*), galactosyltransferase domain (*blue*), β3-glycosyltransferase motifs (*orange*). GalTase, galactosyltransferase.

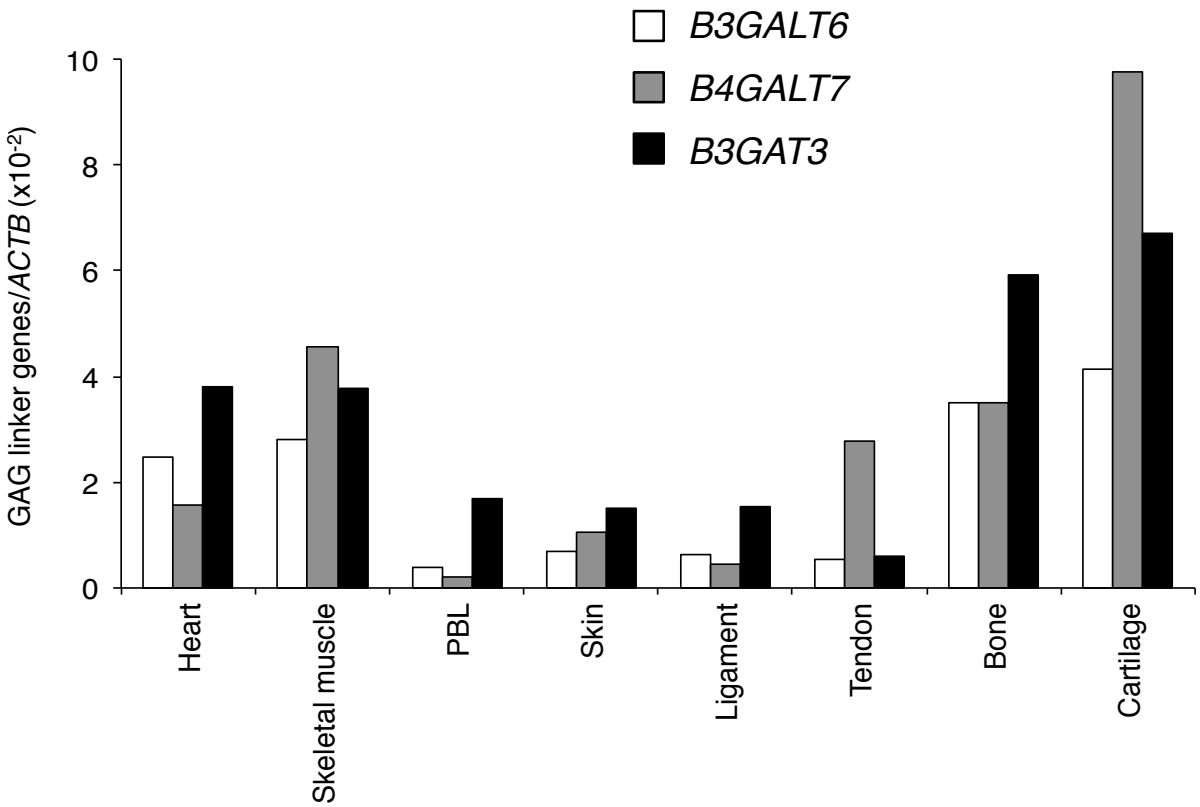

Figure S6. Expression of the GAG linker genes (*B3GALT6, B4GALT7* and *B3GAT3*) mRNAs in human tissues determined by the real-time PCR analysis

The three genes are broadly expressed with slightly different tissue-specificity patterns. Expression of the three genes are strong in cartilage, while their expression in skin, ligament and tendon are weak. The expression of *B4GALT7* in cartilage relative to other tissues is higher in comparison to those of *B3GALT6* and *B3GAT3.* PBL: peripheral blood leukocyte.

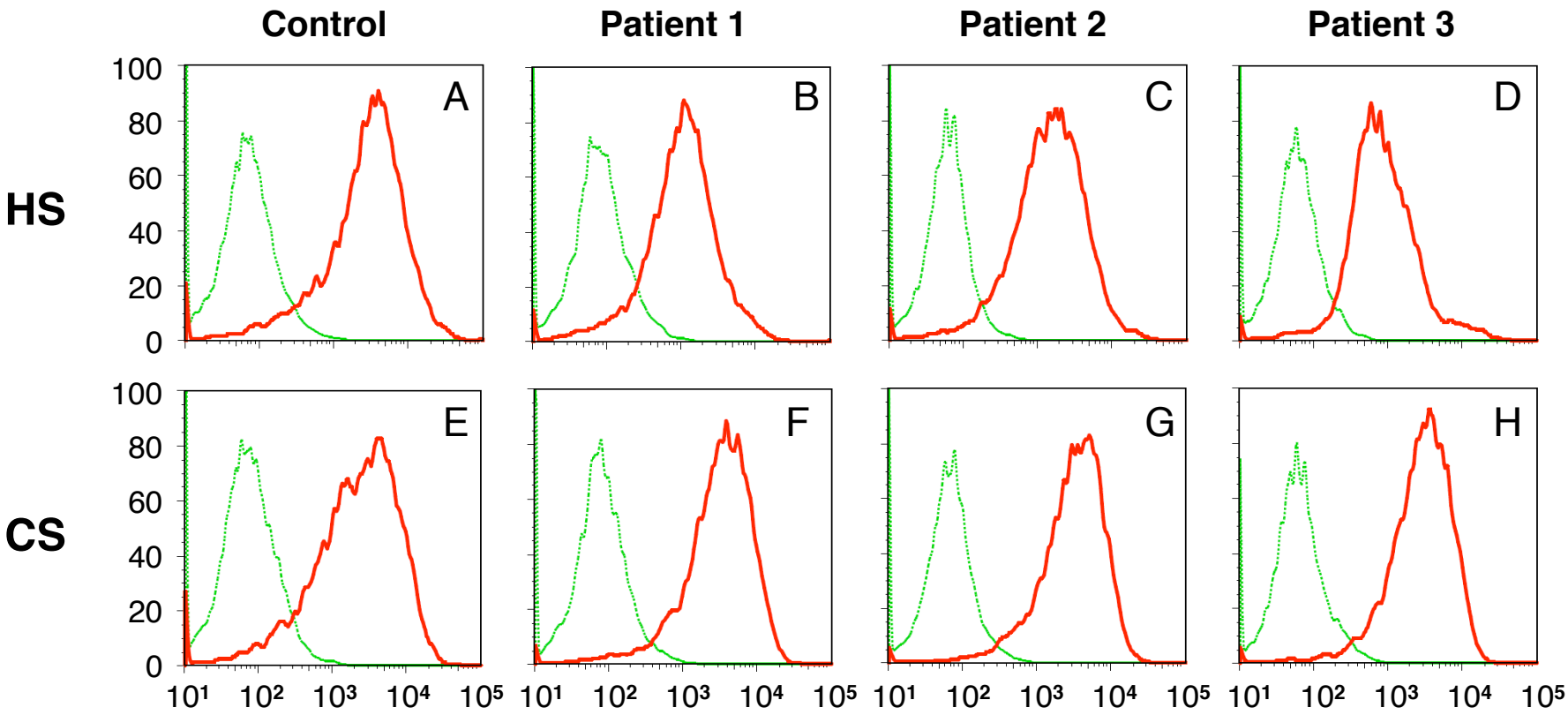

Figure S7. Relative numbers of heparan sulfate (HS) and chondroitin sulfate (CS) chains in individuals with *B3GALT6* mutations

A flow cytometry for the expression of HS (**A**-**D**) and CS (**E**-**H**) at the surface of lymphoblastoid cells. Horizontal axis: fluorescence intensity; vertical axis: relative cell number. **A**, **E**: control; **B**, **F**: Patient 1; **C**, **G**: Patient 2; **D**, **H**: Patient 3. For HS, the cells were treated with a mixture of heparinases-I and –III and then with anti-stub 3G10 antibody in HS; and for CS, with a chondroitinase ABC and then with anti-stub 2B6 antibody. The binding of the antibody to the epitopes was visualized after incubating with an Alexa Fluor 488-conjugated secondary antibody. The *red* and *green* histograms show the intensity of the fluorescence with or without the anti-stub antibodies, respectively.

Table S1. Summary of the exome sequencing performance

Subject ID	No. of bases covered	Average depth of coverage	% of bases above 10x coverage	% of bases above 20x coverage
P1	4,743,306,135	141.7	94.8	91.1
P2	4,994,081,669	149.2	94.9	91.5
P3	3,697,409,162	110.5	93.9	88.5
P4	4,326,027,309	129.2	94.8	91.3
P5	4,433,501,338	132.5	94.8	91.5
P6	4,396,751,708	131.4	94.8	91.5
P7	4,519,248,092	135.0	94.8	91.5
Mean	4,444,332,202	132.8	94.7	91.0

Table S2. ***B3GALT6*** **mutations identified in the individuals with spondyloepimetaphyseal dysplasia with joint laxity type 1 (SEMD-JL1) by exome sequencing and Sanger sequencing**

Mutation		Subject							
Nucleotide change	Amino acid change	P1	P2	P3	P4	P5	P6	P7	P8
		Exome							Non-exome
c.1A>G	p.Met1?	✓	✓	✓	✓	✓		✓	
c.193A>G	p.Ser65Gly							✓	
c.200C>T	p.Pro67Leu								✓
c.466G>A	p.Asp156Asn			✓					
c.694C>T	p.Arg232Cys	✓	✓			✓	✓		✓
c.899G>C	p.Cys300Ser						✓		

gray box: exome sequencing; checked box: Sanger sequencing. P1 and P2 are sibs.